Supplementary Information: Conversion between Two Triplet Pair States Controlled by

Molecular Coupling in Pentadithiophene Thin Films

Natalie A. Pace,[1] Brandon K. Rugg,[1] Christopher Chang,[1] Obadiah G. Reid,[1,2] Karl J. Thorley,[3]

Sean Parkin,[3] John E. Anthony,[3] Justin C. Johnson,[1]

[1]National Renewable Energy Laboratory, 15013 Denver West Parkway, Golden, Colorado

80401, USA

[2]Renewable and Sustainable Energy Institute, University of Colorado Boulder, Boulder,

Colorado 80309, USA

[3]Department of Chemistry, University of Kentucky, Lexington, KY 40506, USA

*Corresponding author email address: Justin.Johnson@nrel.gov

1. Pairwise Crystal Structure

Pairs of TIPS PDT molecules are significantly farther apart from each other (~8.5 Å between acene cores) than pairs of TSPS PDT molecules or TSBS PDT molecules (~3.7-3.9 Å between acene cores in both cases). TIPS PDT molecules are significantly offset along both their long-axis (~4.3 Å) and short-axis (~6.7 Å), whereas TSPS PDT and TSBS PDT are only significantly offset along their long axes (~8.4 Å). Some slip-stacking is favorable for singlet fission (SF), such as that observed along the short axis in TSPS PDT and TSBS PDT crystals (1). However, a large amount of slip-stacking along multiple axes, such as that observed in the TIPS PDT crystal, reduces the orbital overlap needed for a large SF electronic matrix element (1).
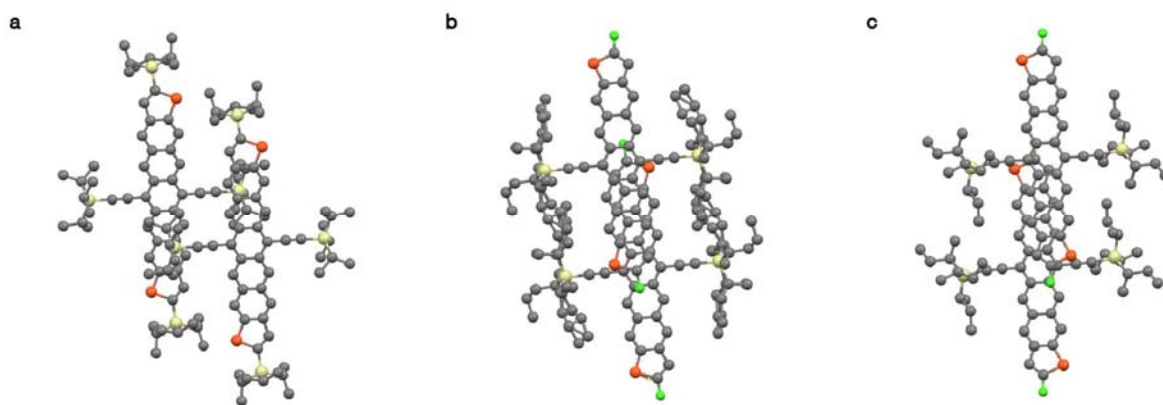

Figure S1: *Arrangements of closest molecular pairs in the crystal structures of (a) TIPS PDT (b) TSPS PDT and (c) TSBS PDT.*

2. Thin Film Steady-State Fluorescence

Fluorescence for the TSPS and TSBS PDT films was weak and difficult to separate from scattering and noise inherent in the detection system at the edge of the instrument sensitivity (900-1050 nm). The TIPS PDT film had weak but detectable emission (Figure S2), most likely prompt emission occurring within the $(TT)_A$ formation time, which was much longer than for TSPS and TSBS. This emission spectrum shows vibronic structure and relatively narrow bands.
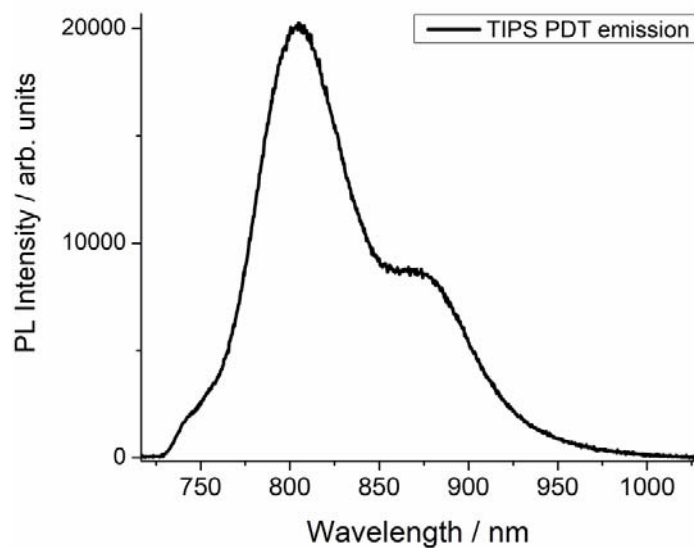
Figure S2. *Steady-state emission of a TIPS-PDT thin film after 700 nm excitation.*

3. Thin Film Crystallinity

As-cast and solvent-annealed TIPS PDT films are prepared via the same spin-casting method. The only difference is an additional annealing step with dichloromethane (12 hours) for the solvent-annealed film. The initial TIPS PDT film is largely amorphous, while the secondary annealing step induces the formation of crystals (Figure S3a). The dataset for the solvent-annealed film is used in the main text in order to compare spectra specifically associated with crystals in different types of PDT films. Both as-cast and solvent-annealed TIPS PDT films exhibit similar dynamics, as determined by SVD and global fit (see Supplementary Section 3). Decay of S_1/formation of $(TT)_A$ occurs in 2.6 ± 0.9 ps and 4 ± 2 ps in the as-cast and solvent-annealed films respectively, decay of $(TT)_A$/formation of $(TT)_B$ occurs in 35 ± 5 and 50 ± 20 ps in the as-cast and solvent-annealed films respectively, and $(TT)_B$ decays on a timescale >5 ns in both films. However, the spectra associated with $(TT)_A$ and $(TT)_B$ are significantly different. The

peaks for both species narrow significantly and increase in intensity by a factor of four in the

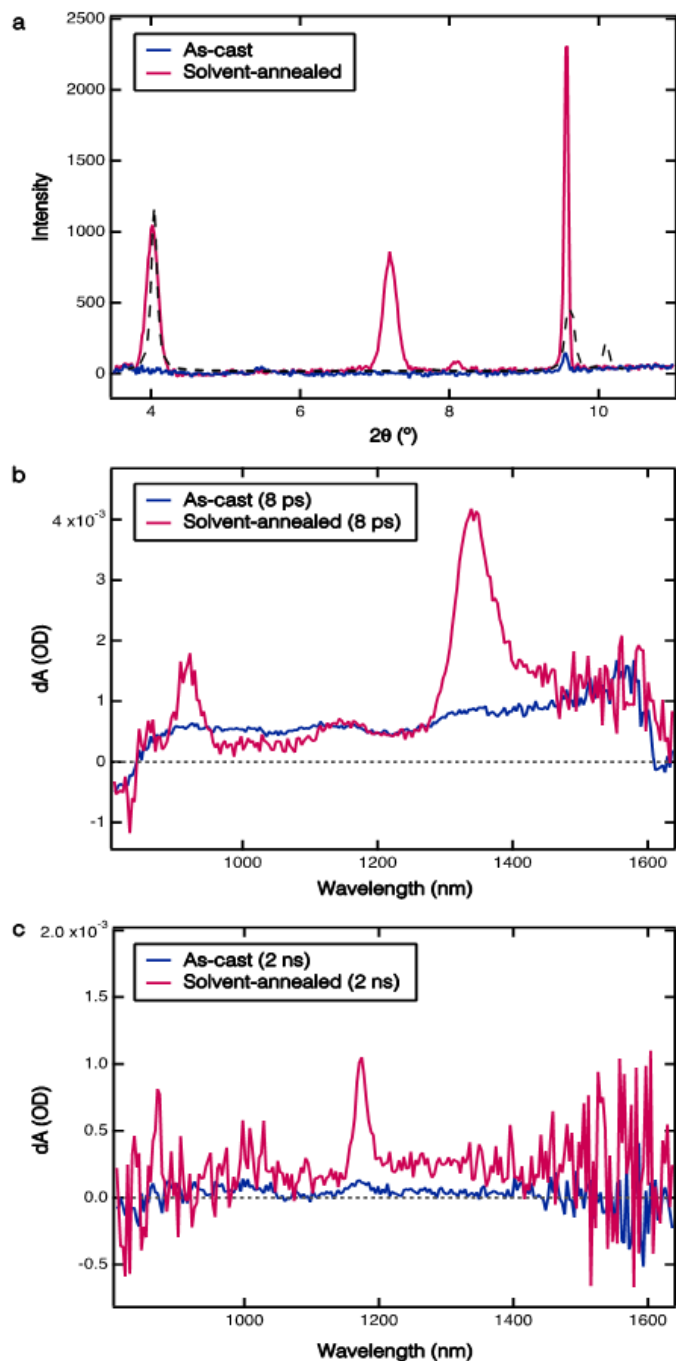solvent-annealed film compared to the as-cast film.

Figure S3*: (a) X-ray diffractograms for as-cast and solvent-annealed TIPS PDT films. Dashed curve is predicted powder pattern. Corresponding near-IR TA spectra for both films at (b) 8 ps and (c) 2 ns. TA spectra normalized to account for a small initial difference in absorbed photon fluence.*
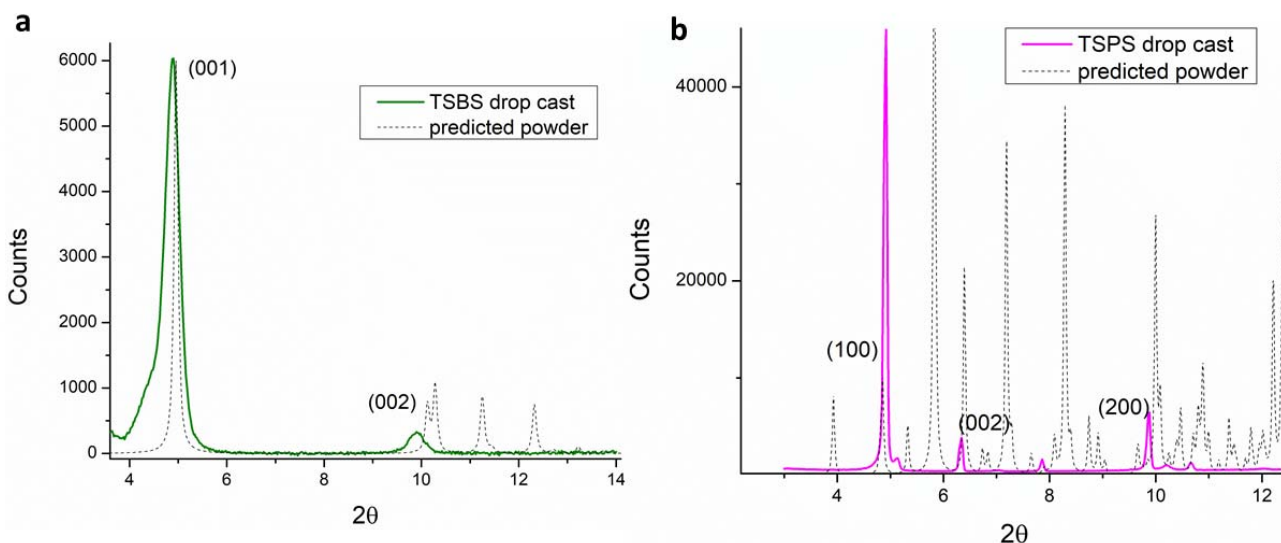
Figure S4. *XRD of drop-cast thin films of (a) TSBS PDT and (b) TSPS PDT. Predicted powder patterns from the known crystal structures are shown as dashed lines, and assignments of reflection planes are included for major peaks. Annealing caused minor sharpening and strengthening of peaks but otherwise similar diffraction patterns.*

4. Transient Absorption in Solution

All three PDT molecules have photoinduced absorption (PIA) features at ~565 nm, ~980 nm, ~1270 nm, and ~1570 nm (Figure S5). The TSPS PDT and TSBS PDT solutions have more prominent bleach features than the TIPS PDT solution in the 650-800 nm region, which are accompanied by a stimulated emission feature at ~850 nm. The TIPS PDT singlet state decays on a ~1-2 ns timescale, while the TSPS PDT and TSBS PDT singlet states decay on a ~5 ns timescale.
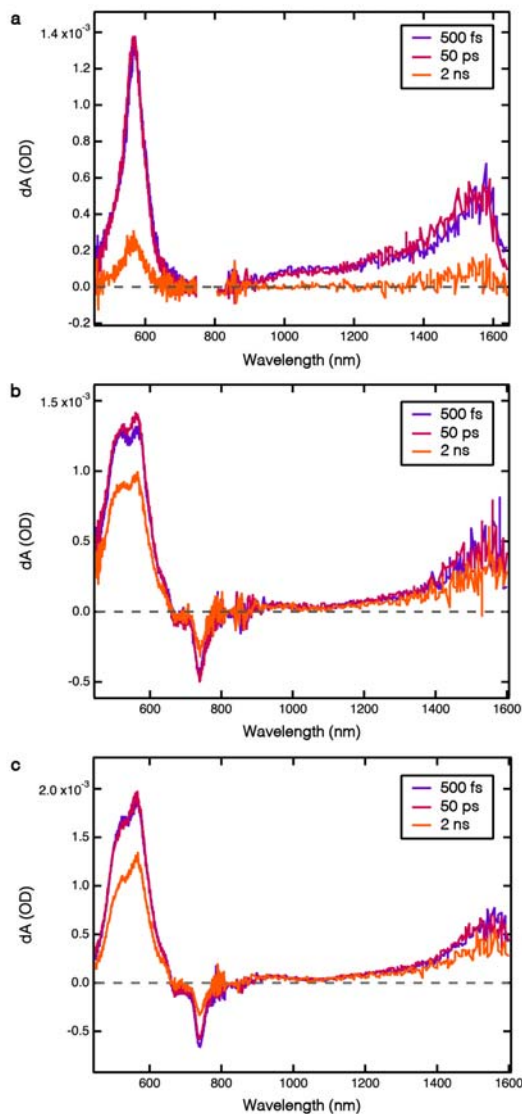
Figure S5*: Solution TA spectra for (a) TIPS PDT, (b) TSPS PDT, and (c) TSBS PDT.*

5. Lifetime of (TT)$_B$

We use kinetic slices at 593 nm to determine the lifetime of the (TT)$_B$ state in each thin film, where the feature at 593 nm represents the general triplet population, and the feature at 1000 nm represents the (TT)$_B$ state specifically (Figure S11). Kinetic traces collected at 1000 nm (not shown) were found to follow the same kinetics but with lower signal. The (TT)$_B$ lifetimes in

the three films differ by more than one order of magnitude, with a time constant of 1.3 ± 0.1 μs

in the TIPS PDT film, 40 ± 2 ns in the TSPS PDT film, and 50 ± 0.07 ns in the TSBS PDT film.
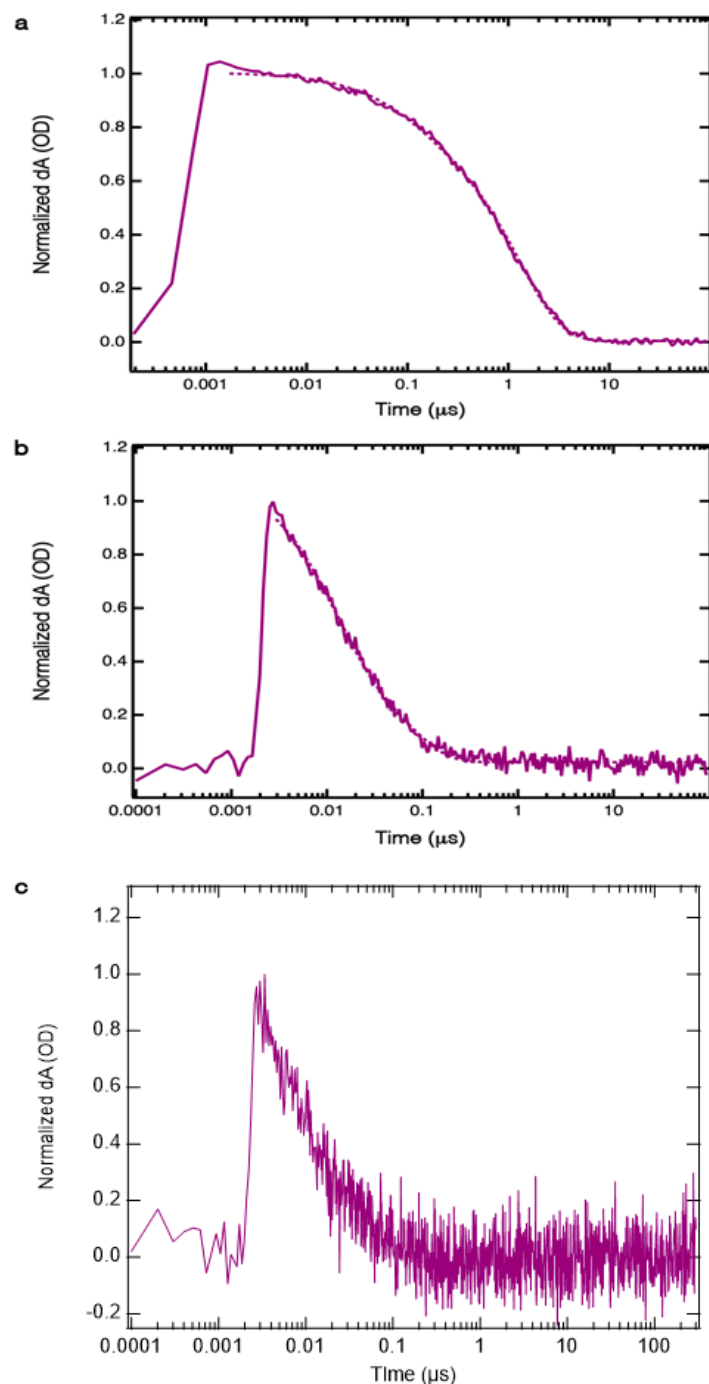

Figure S6: *Kinetic slices at 593 nm (representative of general triplet population) from (a) TIPS PDT (b) TSPS PDT and (c) TSBS PDT thin films. In order to effectively measure the lifetimes of the long-lived species TA data was collected using an electro-optical system (EOS) for detection.*

6. Singlet and (TT)$_A$ Decay in TSPS PDT

Singlet PIA (1400 nm slice) decays on an instrument response-limited timescale ($\leq$ 300 fs) in TSPS PDT films (Figure S7). This decay is accompanied by an initial rise in (TT)$_B$ PIA (~1010 nm). However, after the singlet state has decayed, broad PIA between 1300-1600 nm remains, along with PIA at ~890 nm. This PIA is distinct from both the singlet and (TT)$_B$, and decays with a time constant of 17 $\pm$ 6 ps. This decay is accompanied by a secondary rise in (TT)$_B$ on a timescale of 10 $\pm$ 2 ps. We tentatively assign this intermediate state to (TT)$_A$, given its kinetic and general spectral similarities to the (TT)$_A$ state observed in TIPS PDT. However, the (TT)$_A$ spectrum in TSPS PDT is significantly broader than the "(TT)$_A$" species in TIPS PDT, such that exact peak positions cannot be compared, and a definitive assignment cannot be made. We note that the apparent time constant for (TT)$_A$ decay is slightly longer than the (TT)$_B$ rise because the (TT)$_B$ spectrum also possesses some PIA at 1400 nm. This makes it more difficult to discern an accurate (TT)$_A$ decay time. Therefore, the rise of (TT)$_B$ (10 $\pm$ 2 ps) is likely a more accurate estimate of the conversion time between the two states.
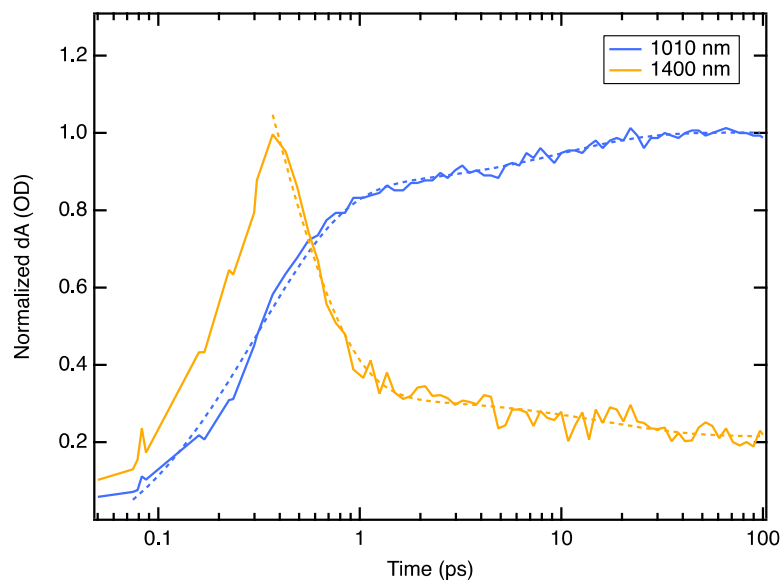

Figure S7*: Kinetic slices from TSPS PDT film TA. The kinetic slice at 1400 nm represents the dynamics of both the singlet state (early times), and the "(TT)$_A$" state (late times). The kinetic slice at 1010 nm represents the dynamics of (TT)$_B$ formation (after 1 ps).*
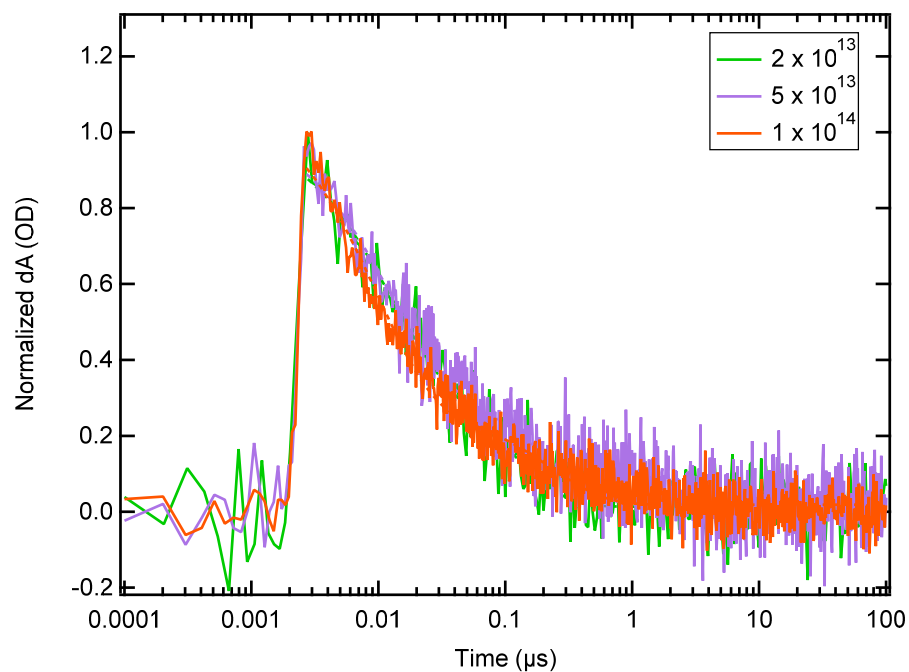
7. TSPS PDT Fluence Dependence

Figure S8*. Fluence dependence of triplet decay at 600 nm for TSPS PDT film.*
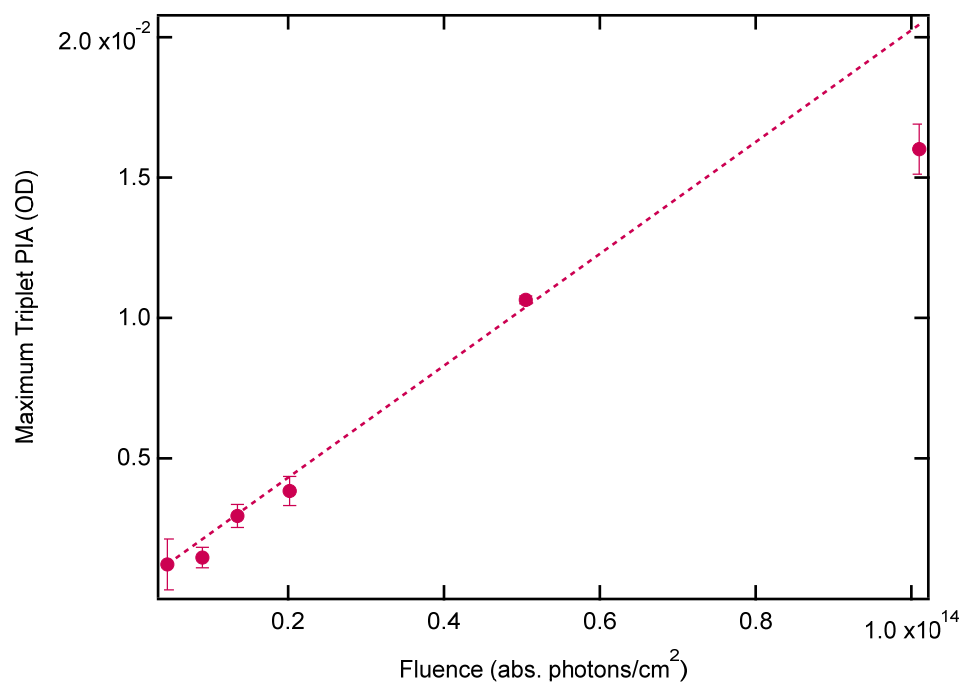

Figure S9*: TSPS PDT maximum triplet PIA (595 nm) as a function of fluence. 700 nm excitation.*
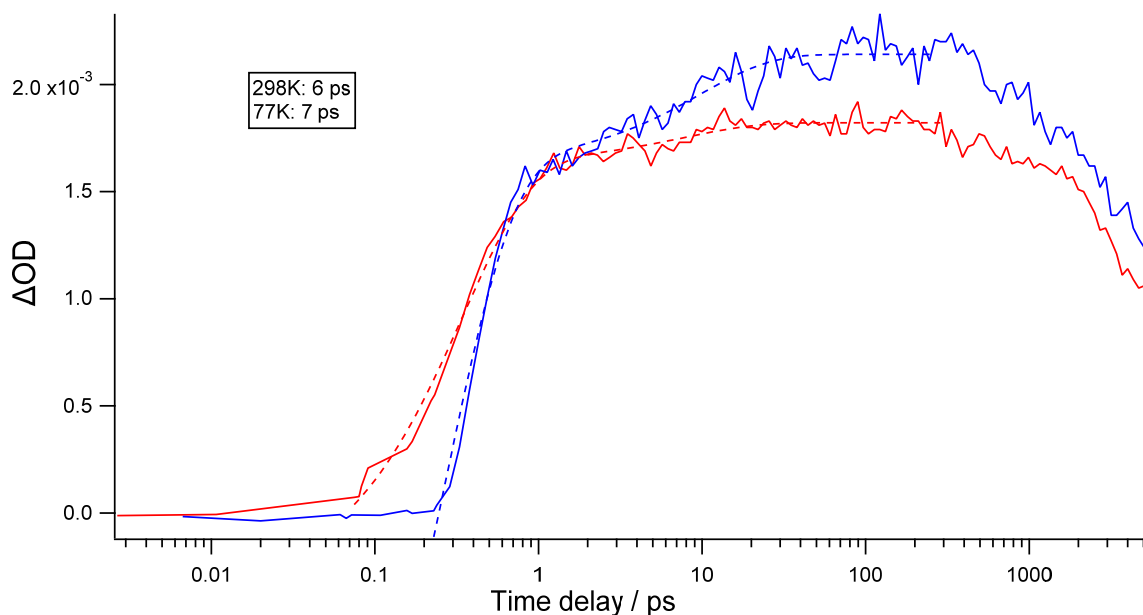
8. TSPS temperature dependence

Figure S10. *Rise of 595 nm feature from transient absorption of TSPS PDT film at 77K (blue) and 298K (red). Secondary rise time constants are shown in the inset and fits are shown as dashed curves. Curves are normalized by the initial rise amplitude (~1 ps).*

9. Singlet and (TT)$_A$ Decay in TSBS PDT

The same general trends are observed in the TSBS film and in TSPS films. The singlet state decays on an instrument response-limited timescale (≤ 300 fs) (Figure S10). The "(TT)$_A$" spectrum is very similar between TSPS PDT and TSBS PDT films, though the decay of this state (10 ± 4 ps) and the rise of the (TT)$_B$ spectrum (3 ± 1 ps) occur on a faster timescale. Again, there is a mismatch between the 1400 nm decay and 1030 nm rise. Since the 1030 nm rise is more spectrally isolated, this estimate for the conversion time is likely more accurate.
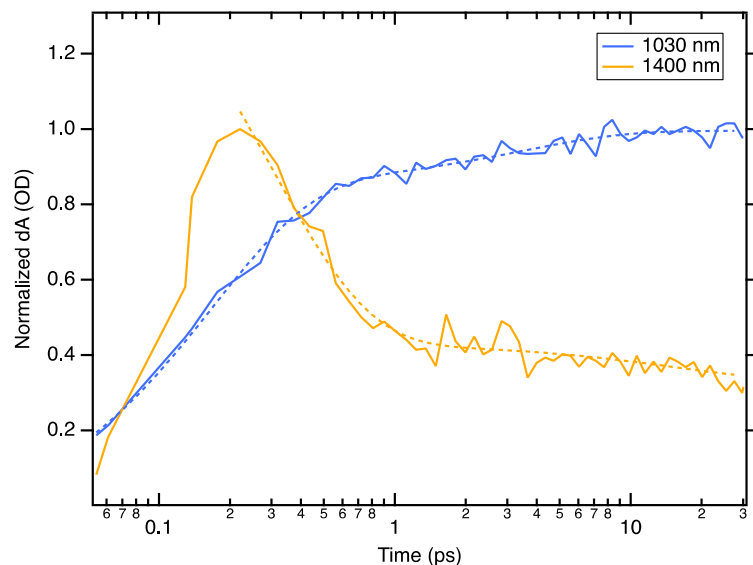
Figure S11*: Kinetic slices from TSBS PDT film TA. The kinetic slice at 1400 nm represents the dynamics of both the singlet state (early times), and the "(TT)$_A$" state (late times). The kinetic slice at 1030 nm represents the dynamics of (TT)$_B$ formation (after 1 ps).*
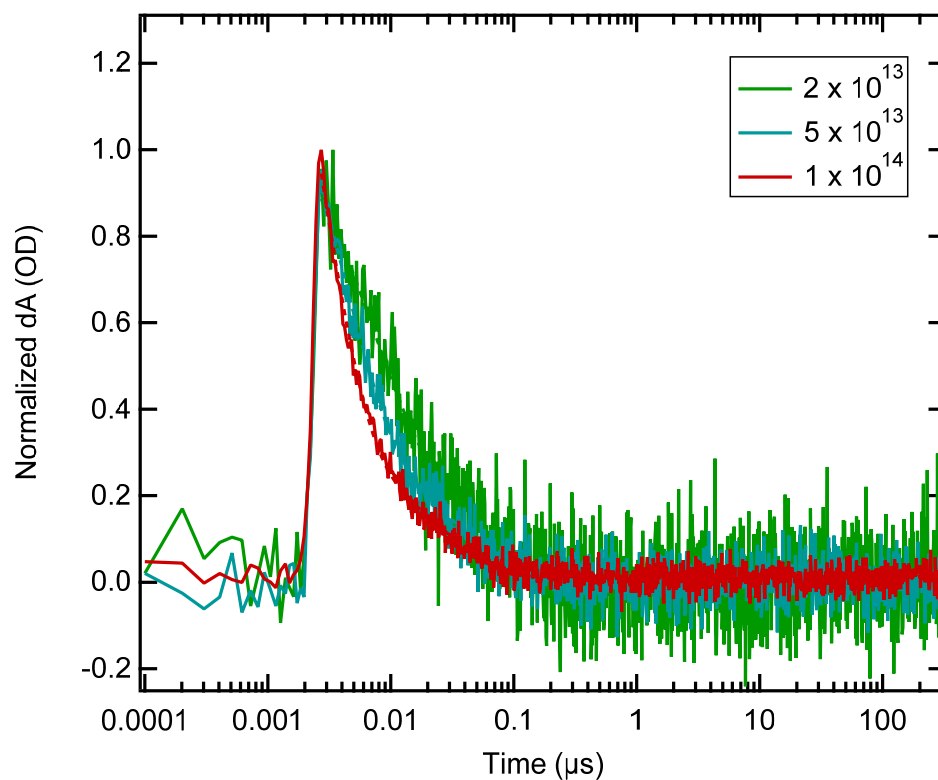

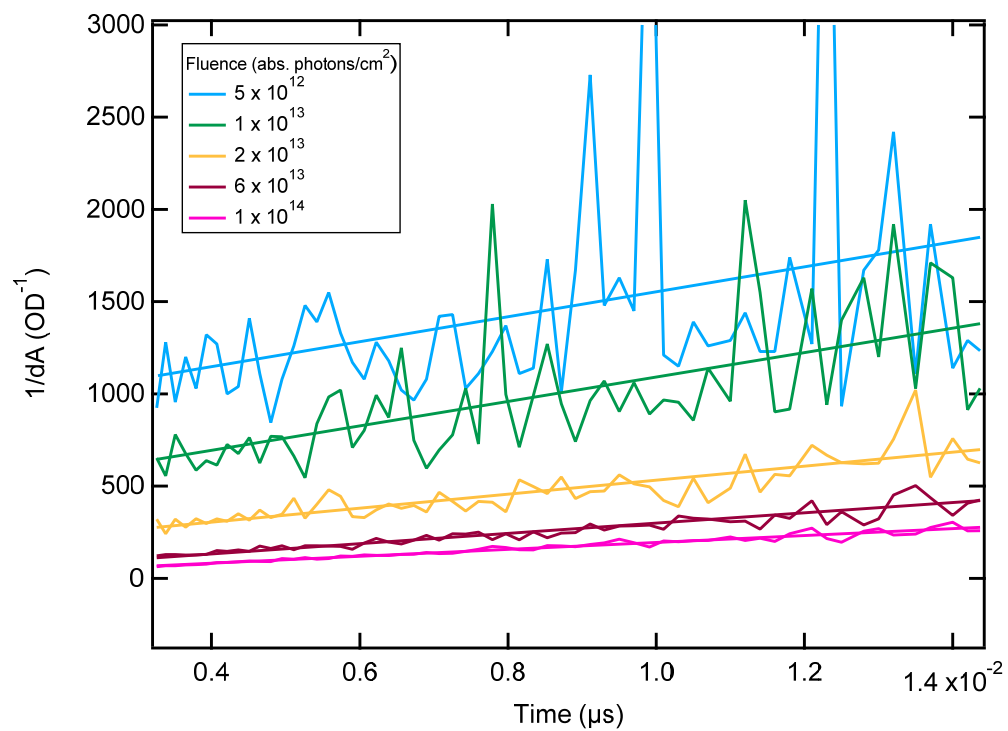***Figure S12****. Fluence dependence of triplet decay at 600 nm for TSBS PDT film.*

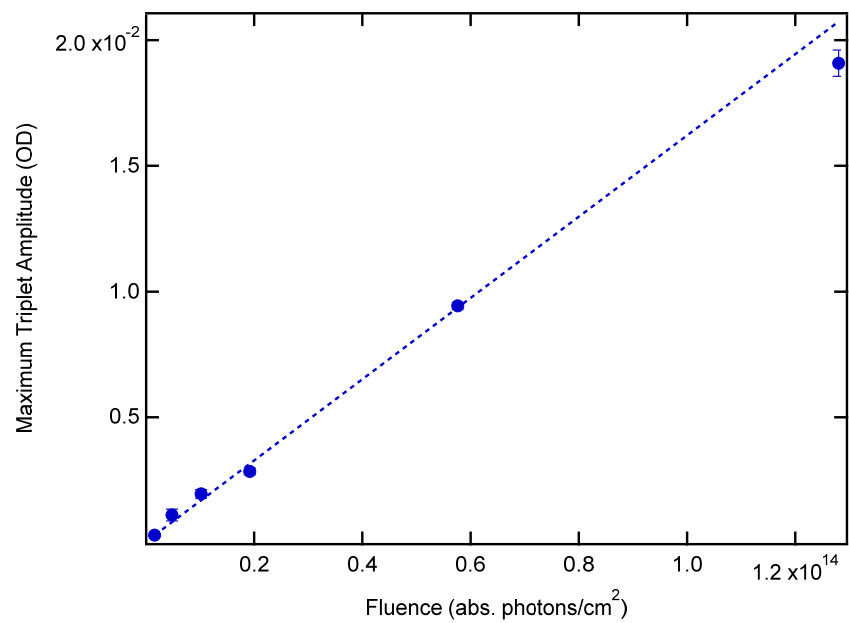**Figure S13**. *Bimolecular decay rate analysis for a TSBS PDT film at various fluences.*

Figure S14: *TSBS PDT maximum triplet PIA (595 nm) as a function of fluence. 700 nm excitation.*

13. TSBS temperature dependence
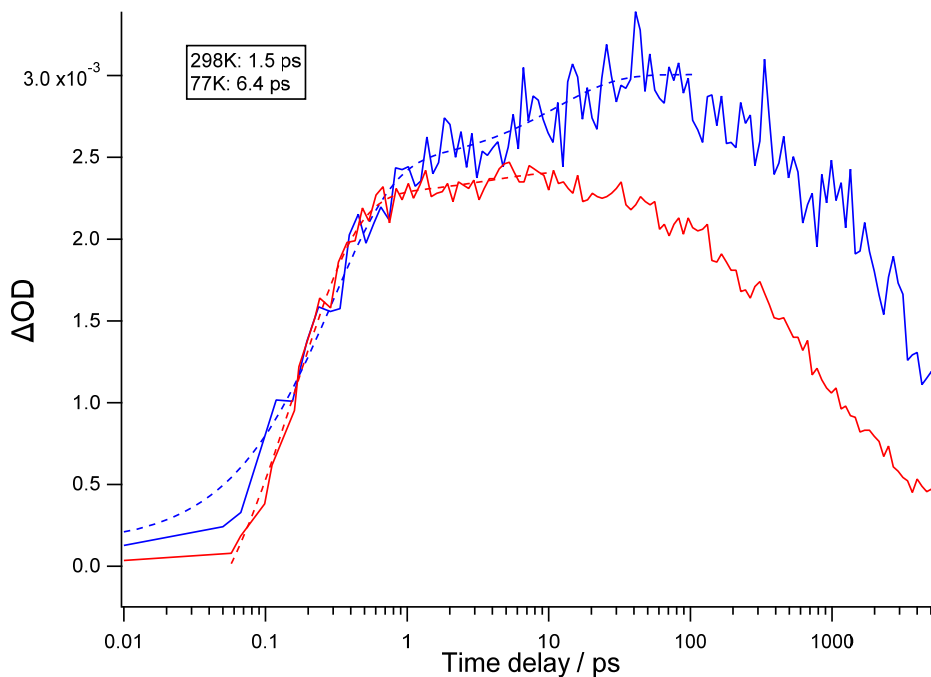
Figure S15. *Rise of 595 nm feature from transient absorption of TSBS PDT film at 77K (blue) and 298K (red). Secondary rise time constants are displayed in the inset and fits are shown as dashed curves. Data are normalized by the initial rise amplitude (~1 ps).*

10. TIPS PDT Fluence dependence

Interestingly, there is no evidence of triplet-triplet annihilation at any fluence for the TIPS PDT film, as the triplet lifetime is fluence-independent (Figure S16) even beyond 1 μs. Since the triplet lifetime is approximately ~1 μs at every fluence, and the distance between triplets is ~3.8 nm at the highest fluence, the triplet diffusion constant is less than ~2 x 10^{-8} cm^2/s. Thus, it takes at least ~50 ns for a TIPS PDT triplet to make a single hop.

Figure S16: *Fluence dependence of triplet decay at 600 nm for TIPS PDT film. Dashed lines are fits.*

Triplet PIA is linear as a function of fluence below ~1 x 10^{14} abs. photons/cm^2 (Figure S13).

Above ~1 x 10^{14} abs. photons/cm^2, there is some evidence of a sublinear trend indicative of

singlet-singlet annihilation.
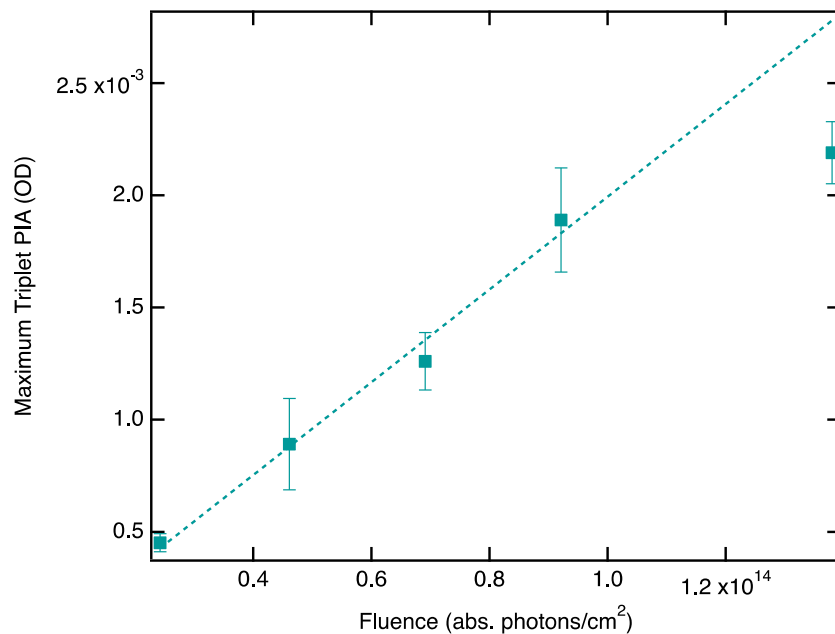
Figure S17: *TIPS PDT maximum triplet PIA (595 nm) as a function of fluence. 700 nm excitation.*
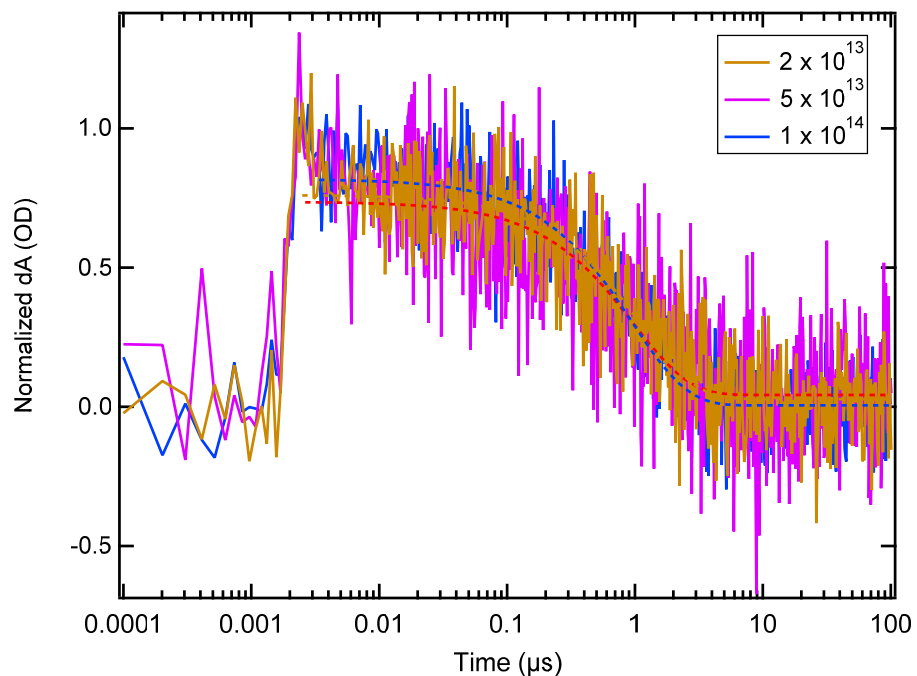
11. TIPS PDT Temperature Dependence

Transitions from ~1200-1500 nm are more sensitive to temperature than other transitions in the near-IR for both (TT)$_A$ and (TT)$_B$ species (Figure S18). At 298 K, the primary transition for (TT)$_A$ in this region (5 ps) is centered at ~1340 nm, with an additional lower-intensity peak at 1260 nm. At 78 K, the oscillator strength of these two peaks is redistributed, such that the peak at ~1260 nm is more intense. The primary transition for the (TT)$_B$ species in this region (300 ps) shifts from ~1340 nm at 298 K to ~1290 nm at 78 K. This (TT)$_B$ transition is therefore distinct from the transition observed at ~1340 nm for (TT)$_A$ at both temperatures. These spectral changes are not accompanied by changes in dynamics (Table S1).

	τ_1	τ_2	τ_3
298 K	3 ± 1 ps	44 ± 6 ps	>5 ns
200 K	2 ± 2 ps	40 ± 10 ps	>5 ns
160 K	2 ± 1 ps	40 ± 10 ps	>5 ns
78 K	2 ± 2 ps	50 ± 30 ps	>5 ns

Table S1: *Time constants from SVD and global fit for decay of S_1/formation of (TT)$_A$ (τ_1), decay of (TT)$_A$/formation of (TT)$_B$ (τ_2), and (TT)$_B$ decay (τ_3) as a function of temperature.*
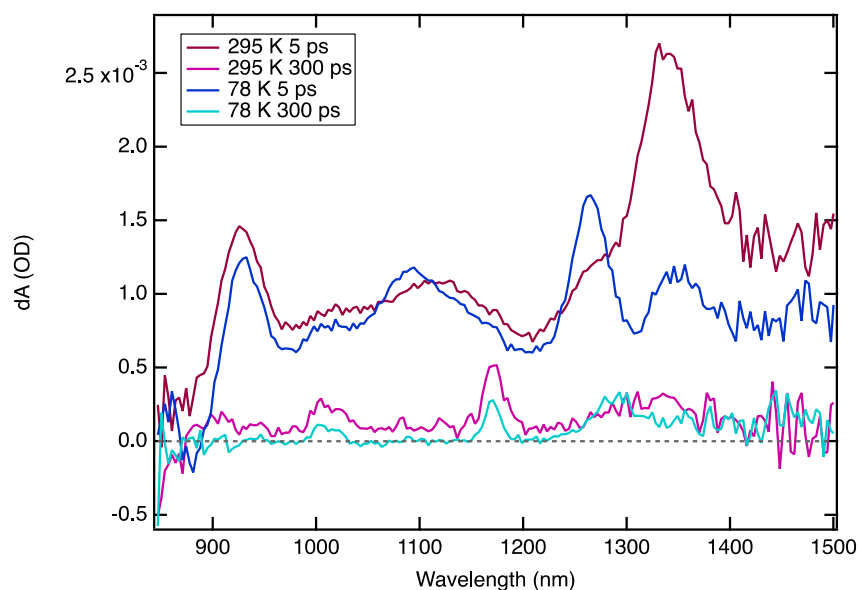
Figure S18: *Comparison between (TT)$_A$ (5 ps) and (TT)$_B$ (300 ps) species for a TIPS PDT film at 295 K and 77 K.*

12. (TT) Transitions in TIPS PDT

Some of the near-IR transitions assigned to the (TT) species in TIPS PDT may belong to the same electronic transition. Deng et. al. observe ring-scissoring modes at ~1700 cm^{-1} in hexacene thin films (2). Similar modes might couple the 11561 cm^{-1} and 9084 cm^{-1} transitions in (TT)$_A$ and the 11494 cm^{-1} and 9804 cm^{-1} transitions in (TT)$_B$ (Table S2). Deng et. al. also observe ring-twisting modes near ~1300 cm^{-1}, which is consistent with the progression we

observe in $(TT)_A$ (1309 cm^{-1}). A similar mode might drive the progression we observe in $(TT)_B$ (1029 cm^{-1}), with a redistribution of oscillator strength between the lower and higher energy transitions.

$(TT)_A$ (cm^{-1})	Δ (cm^{-1})	$(TT)_B$ (cm^{-1})	Δ (cm^{-1})
11561 (w)*		11494 (w)*	
10929 (m)	1757	9804 (m)	1690
9804 (w)		8547 (s)	
8772 (w)		7519 (w)	1028
7905 (m)*	1309		
7463 (s)			

Table S2: *Transitions observed in the near-IR region for (TT) species in TIPS PDT thin films. The strength of each transition is indicated in parenthesis (w= weak, m= medium, s= strong). There is some sample-to-sample variability in the visibility of certain transitions, which makes it difficult to ascertain an accurate peak position to within ± 10 nm. These peaks are marked with an asterisk.*

13. Global Fit of PDT Films

Transient absorption (TA) of the PDT films produces complex dynamics that are difficult to disentangle from kinetic slices. Therefore, we globally fit the data after singular value decomposition (SVD) using a sequential vs. parallel population flow model to further refine the likely kinetic scheme. Distinguishing these pathways results in evolution associated spectra (EAS), which can be turned into population profiles. First comparing the parallel vs. sequential models, we found that the sequential model fit the experimental kinetics faithfully, whereas the parallel fit diverged (Figure S19a). The EAS are shown in Figure S19b. The time constants

obtained from fitting are identical to within uncertainty to those obtained from the exponential
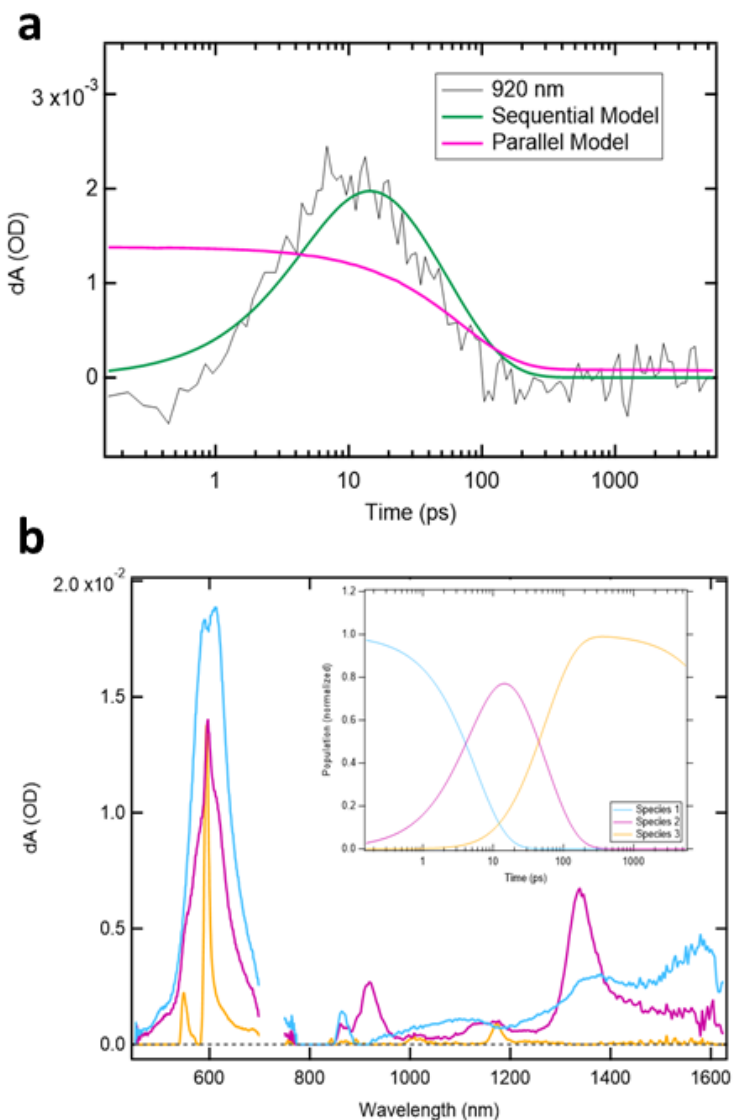
fitting described above.

Figure S19. *A, Fit (bold) vs. experimental kinetics for (TT)$_A$ feature of TIPS PDT film (595 nm). Sequential (green) model is shown to be a more appropriate fit than the parallel (magenta) model. B, Evolution associated spectra resulting from global fit using sequential population scheme. Population profiles are shown as an inset.*

Global fitting of the TA images to specified kinetic models were performed in Igor Pro 6 using a custom code. The fitting procedure is to: (1) Write a set of ordinary differential equations that define the kinetic model; (2) numerically solve the system of equations to obtain population trajectories for all species; (3) fit a linear combination of these (normalized) trajectories to a selection of kinetic slices taken from the TA images; (4) fit the ODE model to the data through iterative repetition of (2) and (3) using a nonlinear least-squares algorithm; (5) use the optimized fit parameters to model the entire TA image, calculate residuals to evaluate the global fit quality, and generate species associated spectra.

The linear combinations of species trajectories are constrained to positive coefficients, and an explicit ground-state population was included in the model to account for negative features. Moreover, for the single negative feature included in the fit (826 nm) only the ground-state population trajectory was allowed in the fit – building in the assumption that this feature is a clean ground-state bleach signature without significant overlap with any excited state absorption features.

Inspection of the TA data suggests the presence of at least three distinct species (S_1, $[TT]_A$, and $[TT]_B$). As such we attempt to fit the data with two different models: sequential and parallel. These models and the corresponding fit parameters are shown in Figure S20. All processes were assumed to be first-order in species concentration. Both the parallel and sequential models fit our data equally well, however there is a great deal more "cross-talk" between the species associated spectra generated using the parallel model. In this case "cross-talk" refers to positive features in one species associated spectrum that appear as negative features in the following spectrum (see Figure S22). Unlike in decay associated spectra, decay and growth of a species are explicitly accounted for in the species associated spectra reported

here and should not show up in spectra associated with two different time constants. Fits to simulated data sets where the exact kinetics are known a-priori show that cross-talk is eliminated if the model is correct. This provides a qualitative indication that the sequential model is a better description of our data.

The fit parameters in Figure S20b and 20d are used to estimate the yield of $[TT]_A$ and $[TT]_B$ species for TIPS PDT. These values of ~10% and ~4%, respectively do not vary substantially between the two models. However, we emphasize that these should be thought of as minimum estimates, as the decay rate constants to the ground state from all species are primarily controlled by the ground-state bleach recovery observed at 826 nm. Any ESA features that overlap with the GSB, particularly those that evolve at later times could mask a substantially higher yield. Similar yield estimates for TSPS and TSBS PDT films give values at or above 100% for $(TT)_A$ and $(TT)_B$, reflecting the lack of the additional decay channel.
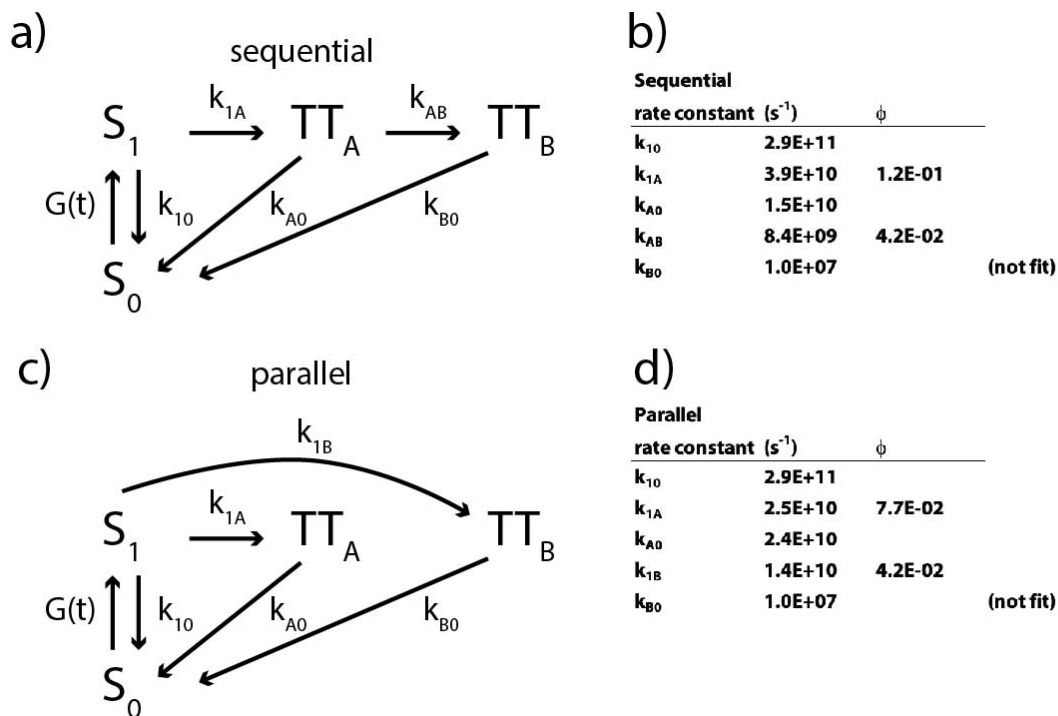
a)

sequential

$$S_1 \xrightarrow{k_{1A}} TT_A \xrightarrow{k_{AB}} TT_B$$

$G(t)$ ↑↓ k_{10} k_{A0} k_{B0}

S_0

b)

Sequential

rate constant	(s^{-1})	ϕ	
k_{10}	2.9E+11		
k_{1A}	3.9E+10	1.2E-01	
k_{A0}	1.5E+10		
k_{AB}	8.4E+09	4.2E-02	
k_{B0}	1.0E+07		(not fit)

c)

parallel

$$k_{1B}$$

$$S_1 \xrightarrow{k_{1A}} TT_A \qquad TT_B$$

$G(t)$ ↑↓ k_{10} k_{A0} k_{B0}

S_0

d)

Parallel

rate constant	(s^{-1})	ϕ	
k_{10}	2.9E+11		
k_{1A}	2.5E+10	7.7E-02	
k_{A0}	2.4E+10		
k_{1B}	1.4E+10	4.2E-02	
k_{B0}	1.0E+07		(not fit)

Figure S20: *a) The sequential kinetic model. b) the best-fit rate constants obtained by fitting the sequential model to the data. c) The parallel kinetic model. d) the best-fit rate constants obtained by fitting the parallel model to the data. In both cases the rate constant for decay of $[TT]_B$ to the ground state was held constant at a quasi-infinite lifetime, as there are some TA features where no decay is observable on the experimental timescale. All other rate constants were freely varied to fit the data.*
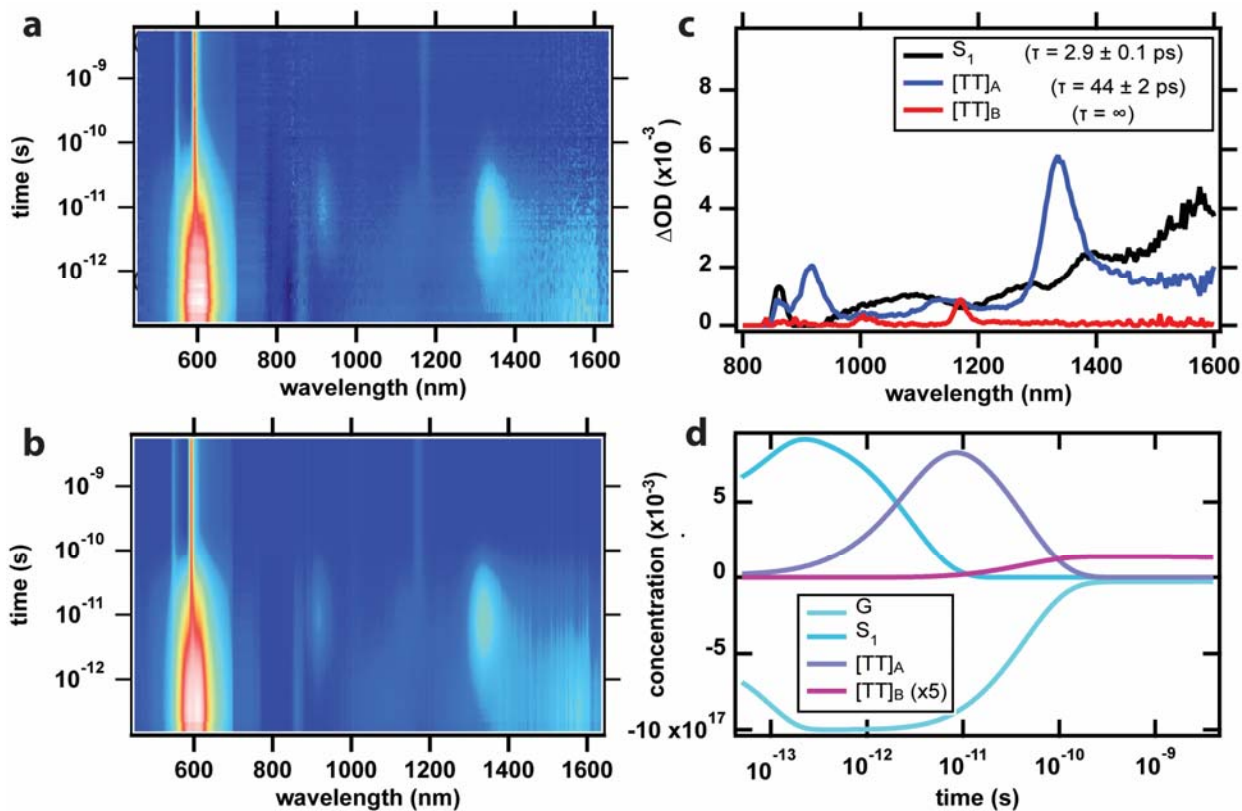
.

Figure S21: *Global fit from sequential kinetic scheme for TIPS PDT film. a) Raw transient data, b) reconstructed data from fit, c) species associated spectra and species decay time constants, and d) concentration profiles.*
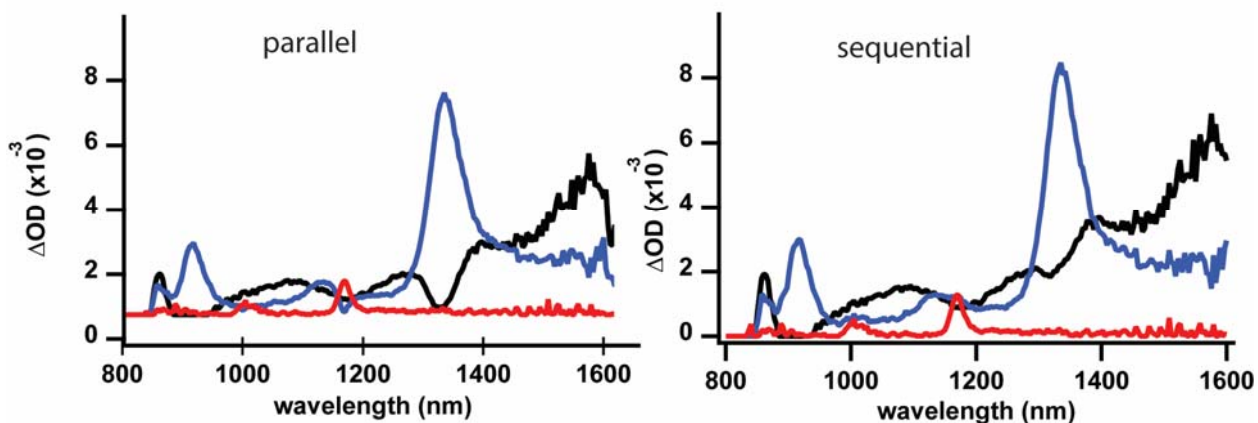

Figure S22: *SADS derived from parallel (left) vs. sequential (right) fits to TA data for TIPS PDT film. Note the exaggerated negative dips mirroring absorptions at 1180 nm (blue curve) and 1330 nm (black curve) for the parallel SADS that are absent in the sequential SADS.*
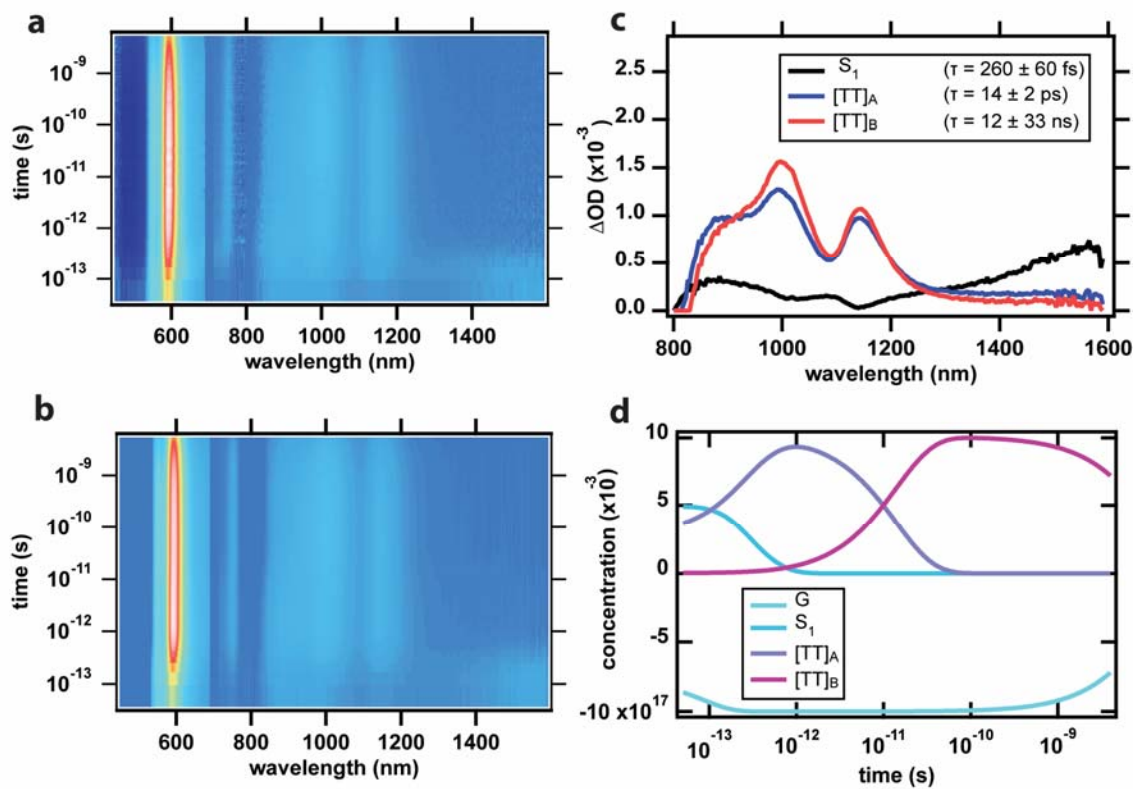
Figure S23*: Global fit from sequential kinetic scheme for TSPS PDT film. a) Raw transient data, b) reconstructed data from fit, c) species associated spectra and species decay time constants, and d) concentration profiles.*

Figure S24*: Global fit from sequential kinetic scheme for TSBS PDT film. a) Raw transient data, b) reconstructed data from fit, c) species associated spectra and species decay time constants, and d) concentration profiles.*
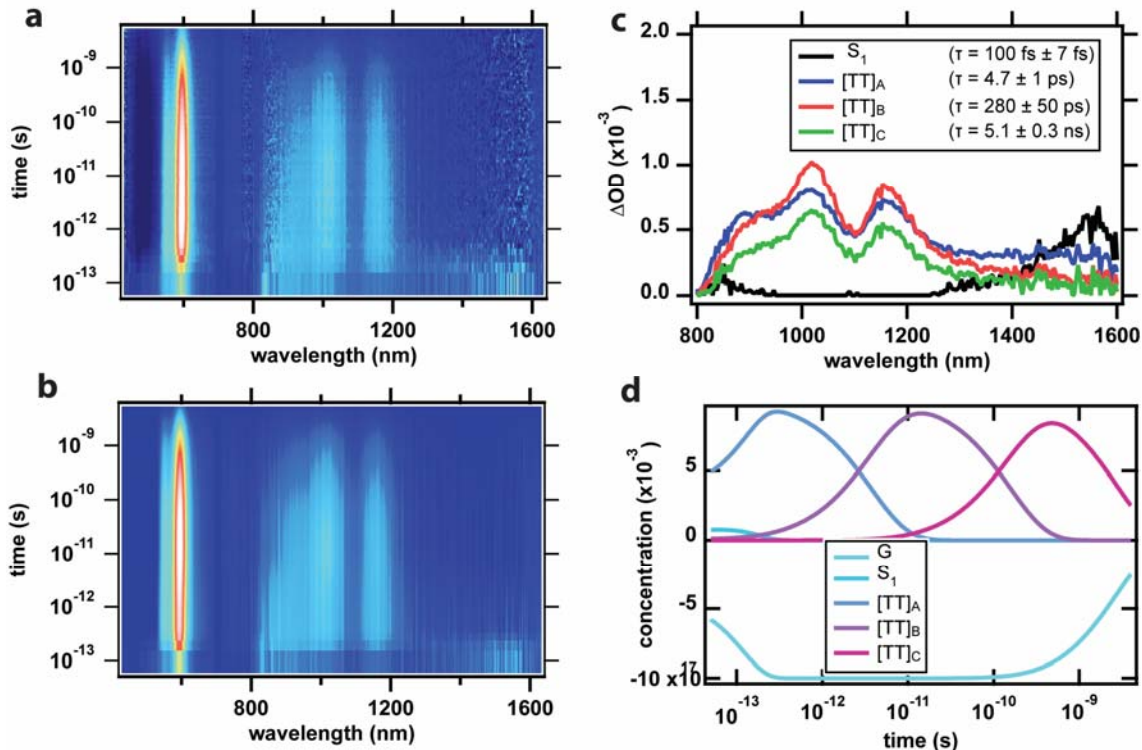
14. EPR details

In order to collect the spectrum of ^{3*}PDT, time-resolved continuous wave EPR (TR-EPR) spectra were obtained at 100 K after photoexcitation (λ_{ex} = 700 nm) of TIPS PDT in a 4:1 solution of 1-iodobutane and toluene. In this solvent mixture, ^{1*}PDT undergoes heavy-atom induced intersystem crossing to form the monomer triplet ^{3*}PDT. The kinetics of these spectra at select field points were globally fit to a single exponential decay (τ = 129 ± 2 ns) convoluted with a gaussian laser pulse envelope and exponential resonator response function. The resulting parameters are D = 1148 MHz, E = 0 MHz, and relative populations of 0.23, 0.38, and 0.39 for the zero field states T_x, T_y, and T_z, respectively.
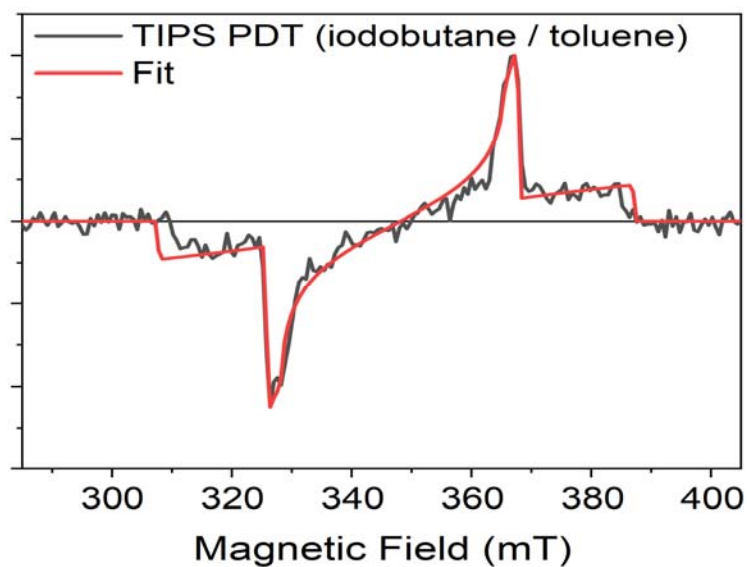
Figure S25. *TR-EPR spectrum of TIPS PDT (black trace) obtained after λ_{ex} = 700 nm in a 4:1 mixture of 1-iodobutane and toluene at 100 K along with corresponding fit (red trace).*
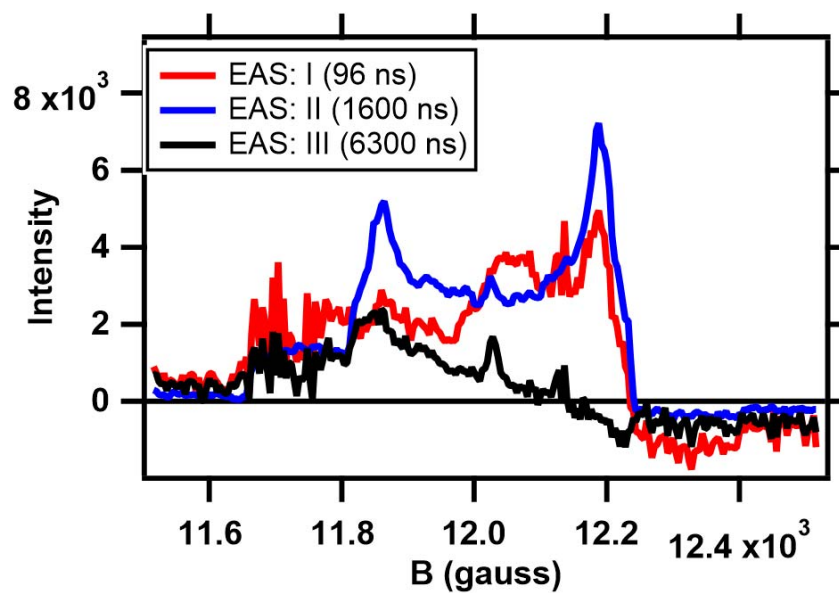

Figure S26. *TR-EPR spectrum of TIPS PDT at Q-band.*
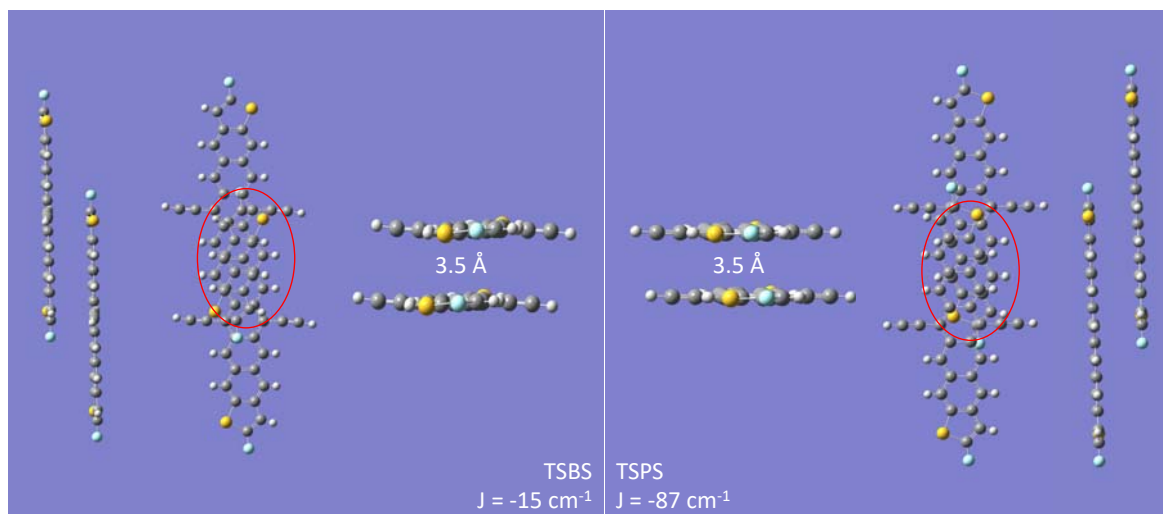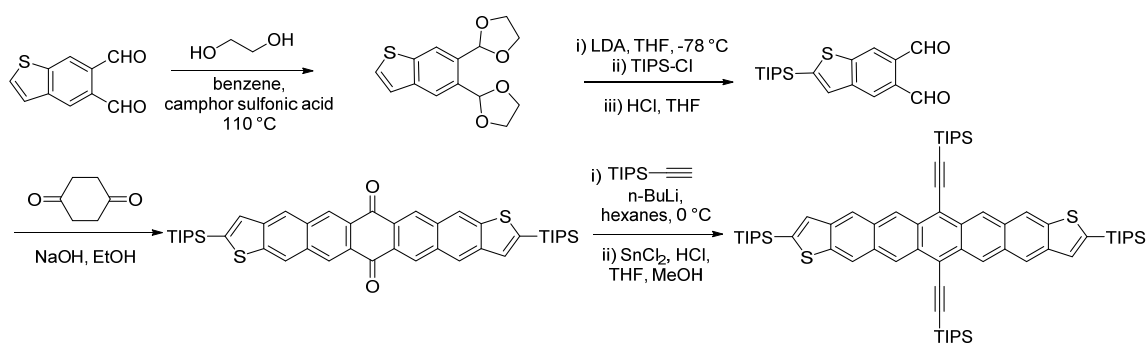
15. Additional Exchange Calculations

Figure S27. *Calculated exchange coupling for TSBS and TSPS "dimers", showing multiple views of intermolecular geometries.*

16. Synthesis of TIPS PDT and TSPS PDT

TIPS PDT:

Benzothiophene-5,6-diacetal: Benzothiophene-5,6-dialdehyde[2] (5.6 g, 29.4 mmol) was dissolved in benzene (100 mL). Ethylene glycol (4.1 mL, 73.6 mmol) and camphor sulfonic acid (0.05 g) were added, and a Dean-Stark apparatus attached to the reaction flask. The mixture was heated at 110 °C for 16 hours. At room temperature, the reaction mixture was diluted with EtOAc (100 mL) and washed with saturated Na_2CO_3 solution (3 x 100 mL). The organic layer

was separated, dried over MgSO$_4$, and the solvent removed. The diacetal was used in the next step without further purification.

2-(tri*iso*propylsilyl) benzothiophene-5,6-dialdehyde: Benzothiophene-5,6-diacetal (4 g, 14.4 mmol) was dissolved in THF (80 mL) and cooled to -78 °C. n-Butyllithium solution (2.5M in hexanes, 6.0 mL, 15.1 mmol) was added slowly, and the mixture stirred for 30 minutes, allowing to warm to room temperature. Tri*iso*propylchlorosilane (3.45 g, 17.9 mmol) was added, and the reaction was stirred at room temperature for 1 hour. The reaction was quenched with 10% HCl solution (20 mL) and diluted with CH$_2$Cl$_2$ (100 mL). The organic layer was washed with H$_2$O (3 x 50 mL), and then the solvent was removed. The crude material was re-dissolved in THF (10 mL) and 10% HCl solution (50 mL) was added. This mixture was stirred vigorously for 16 hours. CH$_2$Cl$_2$ (100 mL) was added, and the organic layer was separated. The mix was passed through a silica plug (CH$_2$Cl$_2$), and then recrystallised from hexanes/EtOAc (5:1) to yield the product as pale yellow crystals (3.2 g, 64 %). ^{1}H NMR (CDCl$_3$, 400 MHz) 10.66 (1H, s), 10.61 (1H, s), 8.51 (1H, s), 8.42 (1H, s), 7.71(1H, s), 1.46 (3H, septet, J = 7.4 Hz), 1.17 (18H, d, J = 7.4 Hz); ^{13}C NMR (CDCl$_3$, 100 MHz), 192.4, 192.1, 147.6, 145.9, 143.5, 133.0, 132.7, 131.5, 127.7, 126.0, 18.5, 11.7; m/z (EI): Found 346.1610 (C$_{19}$H$_{26}$O$_2$SSi requires 346.1422)

diTIPS PDT quinone: 2-(tri*iso*propylsilyl) benzothiophene-5,6-dialdehyde (1.0 g, 2.88 mmol) and 1,4- cyclohexanedione (0.147 g, 1.31 mmol) were dissolved in EtOH (20 mL) with heating. At room temperature, 15% NaOH solution (0.05 mL) was carefully added, and the mixture stirred at room temperature for 1 hour. The mix was filtered and washed with EtOH, acetone,

and Et$_2$O to give the quinone as an insoluble dark orange solid (0.51 g, 53 %). Further characterization was not possible due to poor solubility.

TIPS PDT: Triisopropylsilyl acetylene (0.76 mL, 3.4 mmol) was dissolved in hexanes (40 mL) and cooled to 0 °C. n-Butyl lithium (2.5 M in hexanes, 1.09 mL, 2.73 mmol) was added and the reaction mixture stirred at 0 °C for 1 hour. diTIPS PDT quinone (0.5 g, 0.68 mmol) was added and the reaction stirred overnight at room temperature. The reaction was quenched by addition of a few drops of saturated NH$_4$Cl solution. The crude mixture was poured onto a silica plug and eluted with hexanes to recover excess silyl acetylene, then CH$_2$Cl$_2$/acetone (1:1) to recover the PDT diol intermediate. After removal of CH$_2$Cl$_2$ and acetone, the diol was redissolved in THF (5 mL) and MeOH (25 mL). Tin(II) chloride (0.77 g, 3.4 mmol) and 10% HCl solution (5 mL) was added, and the mixture stirred for 1 hour. The solvent was removed and the mixture was passed through a silica plug with hexanes. Recrystallisation from toluene gave the TIPS4 PDT as dark green crystals (0.055 g, 8 %). ^{1}H NMR (CDCl$_3$, 400 MHz) 9.49 (2H, s), 9.38 (2H, s), 8.44 (4H, s), 7.53 (2H, s), 1.39-1.49 (52H, m), 1.21 (38H, d, J = 7.6 Hz). ^{13}C NMR (CDCl$_3$, 100 MHz), 141.9, 141.8, 141.6, 132.2, 119.7, 19.1, 18.7, 11.8, 11.8. m/z HRMS (LDI-TOF): found 1062.6051 (C$_{66}$H$_{94}$S$_2$Si$_4$ requires 1062.5874).

TSPS PDT*:*
To a dry 50 mL round-bottom flask was added 6 mL of hexanes and tri(2-pentyl)silyl acetylene (0.584 g, 2.19 mmol). The solution was cooled to 0°C and a 2.5 M solution of n-BuLi in hexanes (0.79 mL, 2.0 mmol) was added dropwise. After 1 hour, difluoro-pentadithiophenequinone (200 mg, 0.438 mmol) was added along with 10 mL hexanes and 6 mL of THF. The next day, an

additional 6 mL of THF was added and stirred another few hours. The reaction was poured through a thin silica gel plug and flushed with THF. Solvent was removed through rotary evaporation. The mixture was eluted through a silica gel plug with hexanes to remove excess alkyne followed by 1 hexanes : 1 dichloromethane and then pure dichloromethane to elute diol mixture. Solvent was removed by rotary evaporation and solids were dissolved in ~25 mL acetone. $SnCl_2 \cdot 2\ H_2O$ (0.14 g) and ~ 0.5 mL 10% HCl were added to make a dark green solution of product. After TLC showed the reaction was complete, it was filtered and the solids purified on a silica gel plug with hexanes to give ~40 mg of product. This was recrystallized in ~1 mL of hexanes to give 27 mg of product, 6% yield. X-ray quality crystals were grown by solvent diffusion with $CHCl_3$/MeOH in an NMR tube. ^{1}H NMR (400 MHz, $CDCl_3$) ∂ 9.38 (s, 2H), 9.33 (s, 2H), 8.24 (s, 2H), 8.18 (s, 2H), 6.72 (s, 1H), 6.71 (s, 1H), 1.90 (m, 6H), 1.74 (m, 6H), 1.58 (m, 6H), 1.44 (m, 6H), 1.36 (s, 24H), 1.01 (t, J = 7.2 Hz, 18H). ^{13}C NMR (100 MHz, $CDCl_3$) δ 167.1, 164.1, 136.65, 136.59, 133.6, 130.7, 130.3, 126.3, 125.5, 121.7, 121.5, 118.2, 109.0, 105.2, 102.6, 102.5, 35.22, 35.20, 35.18, 22.1, 16.93, 16.90, 15.48, 15.46, 14.5. MS (LDI) m/z 954.5 (M^+). HRMS (EI) 954.4818 ($C_{60}H_{76}F_2S_2Si_2$ requires 954.4895).

References:

1. E. A. Buchanan, J. Michl, Packing Guidelines for Optimizing Singlet Fission Matrix Elements in Noncovalent Dimers. *J. Am. Chem. Soc.* **139**, 15572–15575 (2017).

2. G.-H. Deng, *et al.*, Vibronic fingerprint of singlet fission in hexacene. *J. Chem. Phys.* **151**, 054703 (2019).

3. M. M. Payne, S. A. Odom, S. R. Parkin, J. E. Anthony, Stable, Crystalline Acenedithiophenes with up to Seven Linearly Fused Rings. *Org. Lett.* **6**, 3325–3328 (2004).